A novel wellbore strengthening method by using rotary jet while drilling

Peng Wang [a,b,c], Hongjian Ni [a,b,*], Haoge Liu [d], Bo Zhao [e]

[a] Key Laboratory of Unconventional Oil & Gas Development (China University of Petroleum (East China), Ministry of Education, Qingdao 266580, China.

[b] School of Petroleum Engineering, China University of Petroleum (East China) Qingdao 266580, China.

c National Engineering Laboratory of Offshore Geophysical and Exploration Equipment, China University of Petroleum, Shandong 266580, China.

[d] Department of Geoscience and Petroleum, Norwegian University of Science and Technology, Trondheim NO-7491, Norway.

[e] Oil Industry Training Centre, China University of Petroleum (East China), Qingdao, China.

∗ Corresponding author at: China University of Petroleum (East China), No. 66, West Changjiang Road, Huangdao District, Qingdao 266580, China. E-mail address: h20160011@upc.edu.cn (H. Ni)

Abstract: Lost circulation is one of the most common and costly problems in drilling operations. Improving the wellbore strengthening by plugging drilling induced fractures using rotary jet method is a novel and effective method to mitigate lost circulation. A stress analysis model based on elastic-plastic mechanics was established to reveal the wellbore strengthening mechanism of rotary jet plugging while drilling. The structure of rotary jet tool was proposed and mixture multiphase flow model was adopted to optimize the structure of the modulation unit of rotary jet. The field tests of engineering prototype were carried out in 8½″ interval of three wells. Satisfactory plugging results verify the effectiveness of rotary jet plugging and wellbore strengthening technology.

Keywords: lost circulation; wellbore strengthening; mechanism; rotary jet; field test

1 Introduction

Lost circulation has been identified as one of the major causes of non-productive time and increase of drilling cost, especially in deep-water drilling (Carpenter, 2014). Reports show that 12% of the non-productive time in shelf drilling of Gulf Mexico was related to lost circulation, which is responsible to 10% to 20% of the cost during the whole drilling cycle (Wang et al., 2019). Worldwide, the impact of lost circulation on well construction is estimated at 2 ~ 4 billion dollars annually in lost productive time, lost drilling fluid, and materials used to prevent the losses (Feng and Gray, 2017). To slove lost circulation problems, the primary considerations are to clog fluid loss channel and prevent fractures from further propagation or strengthen the wellbore wall. Most common plugging and remedial wellbore strengthening involve using particle lost circulation materials in drilling fluid to prop, bridge or seal the fractures by use of lost circulation materials in drilling fluid. According to whether the drilling operation stops during circulating the drilling fluid with particles, these technologies can be divided into two categories: stop-drilling plugging and plugging while drilling. Compared with stop drilling plugging, plugging while drilling tremendously saves the drilling costs and has become a research hotspot in recent years.

Both stop-drilling plugging and plugging while drilling take advantage of the pressure difference between the annulus and the pore pressure of the leakage zone to squeeze the particle materials into the leakage zone. The key issue is whether the size of the material matches the crack size of the leakage zone, which is the reason for many scholars focusing on the formula and interaction mechanisms of particle drilling fluids (Fuh et al., 2007). Due to the randomness of the particle material entering the crack and the speed of the material entering into the crack depending on the pressure difference, the required time and results of plugging are very unstable. For that reason, a reinforcement method of plugging while drilling by utilizing rotary jet to accelerate the plugging agent entering and quickly seal the leakage formation was proposed (see Fig. 1): A rotary jet modulation tool with two nozzles on its side wall is directly mounted over the drill bit. A diffused jet with three-dimensional velocity erupts out the nozzles and accelerates the particle materials in the annulus impacting and entering the leakage formation, so as to realize rapid and efficient sealing of the leakage crack at the crack entrance and further improving the pressure-bearing capacity of the wellbore wall. Compared with straight flow, the rotating jet has the characteristics of larger impact area in a short distance, no center constant velocity core, more uniform pressure distribution, and strong entrainment ability, which are beneficial to protect wellbore wall and sealing the crack.

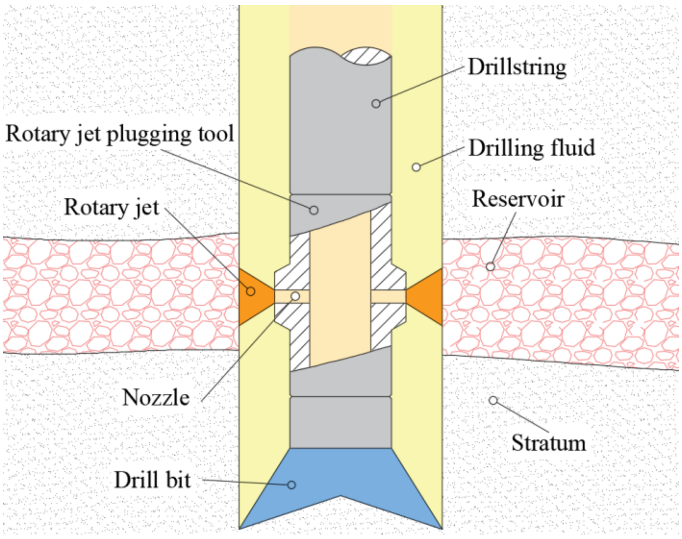

Fig. 1. Schematic diagram of rotary jet plugging technology while drilling.

The main purpose of rotary jet technology while drilling is to strengthen the borehole wall. The wellbore strengthening mechanism is that the particle materials rapidly rush to the crack at different angles and quickly form sealing under the action of rotating jet. Then the crack is widened and the transmission of drilling fluid pressure to the crack tip is effectively isolated and the crack expanding is prevented. There have been a lot of researches on the use of plugging drilling fluid to strengthen borehole wall, mainly focusing on the formula of plugging drilling fluid and the selection and development of plugging materials. However, there is still no consensus on the fundamental mechanisms to explain how wellbore strengthening works. Wellbore strengthening techniques are generally theorized to work by either of the three mechanisms (Feng and

Gray, 2017; Mehrabian et al., 2015).

(a) Fracture propagation resistance: Carefully conducted experimental investigations on lost circulation were conducted, and remarkable enhancements in the pressure-bearing capacity of the wellbore due to wellbore strengthening treatments were observed in the DEA-13 project (Morita et al., 1990; Onyia, 1994), regarding the particle material seals at the tip of crack and proposed fracture propagation resistance theory. Fuh et al. (Fuh et al., 2007; Fuh et al., 1992; Morita and Fuh, 2012; Morita et al., 1988) researched the filtration characteristics of drilling fluid at tip of crack and thought the crack tip would stop extending when the velocity of drilling fluid flowing into the crack tip was less than the velocity of flowing from the crack tip to the reservoir, which was only applicable to the reservoir with high permeability.

(b) Stress cage: With the development of plugging technologies, scholars began to realize that the use of reasonable drilling fluid technology can not only prevent lost circulation, but also strengthen the wellbore. Another experimental effort to investigate lost circulation and wellbore strengthening was the Global Petroleum Research Institute 2000 (GPRI 2000) project conducted in the late 1990's (van Oort et al., 2011), several formulas of drilling fluid were developed to plug up the crack at the entrance of crack and strengthen the wellbore (Sweatman et al., 1999; Sweatman et al., 2004; Sweatman et al., 1997; Wang et al., 2008; Wang et al., 2005; Wang et al., 2007a; Wang et al., 2007b; Whitfill, 2008; Whitfill, 2005; Whitfill and Hemphill, 2003; Whitfill et al., 2007; Whitfill et al., 2006). Alberty and McLean (2001) proposed stress cage theory: the solid phase material in the drilling fluid entered into the crack and formed a blocking barrier near the crack entrance, which could block the transmission of drilling fluid pressure and fluid medium. The pressure in the crack gradually dissipated and finally tended to the pore pressure. The artificial spacer increased the circumferential stress of the wellbore wall while preventing the closure of the crack and strengthened the wellbore at last. Alberty and McLean (2004) used the finite element method to prove the increase of circumferential stress in the surface of crack and stress cage theory was proved to be correct

(c) Fracture closure stress (FCS): Dupriest et al. (2005; 2008) proposed the idea that improving the fracture closure stress was beneficial to wellbore strengthening. Their research suggested that the leakage cannot be controlled effectively by simple plugging, and the solid particle material must isolate the crack tip and sufficient crack width was necessary to obtain to make fracture closure stress higher than equivalent circulating density. Oort (2011) pointed out that the hypothesis of crack length and blockage depth in the stress cage theory lacked theoretical basis, and the FCS theory failed to explain the importance of plugging material strength and the poor treatment effect of low permeability formation. Nair and Abousleiman (2009) summarized the mechanical, thermal and chemical methods for improving the pressure-bearing capacity of the formation and thought the understanding of the mechanism of wellbore strengthening was still vague and the established model could not be widely confirmed by laboratory and field tests.

Other scholars (Green and Sneddon, 1950; Palmer, 1993; Wang et al., 2009) discussed the problems of induced stress field, the non-uniform induced stress of cracks and multiple cracks. It can be seen from the above research on the wellbore strengthening mechanism that fracture propagation resistance theory assumed the solid particle materials sealed at the crack tip, which cannot be met due to the propagation of fluid pressure usually precedes that of fluid medium. Stress cage theory required that the sealing material should have mechanical strength to support the crack to keep open, meanwhile, it was also required that the sealing material could form the isolation layer with very low permeability in a short time. At present, there is no widely accepted theoretical explanation for the mechanism of improving the pressure-bearing capacity of the reservoir. The stress cage theory can explain the mechanism of wellbore strengthening by quickly sealing the crack entrance to some extent. Unfortunately, the presenter of the stress cage effect only put forward the perceptual explanation and its field application effect, but did not give the corresponding mathematical analysis.

This paper focuses on the rotary jet plugging technology while drilling. First, a mathematical model based on stress cage theory was established to analysis the effect of circumferential stress increment on collapse, fracture burst pressures at different positions of wellbore and the mud-weight window (MWW). Second, a structure of rotary jet tool was proposed and mixture multiphase flow model was adopted to optimize the structure of the modulation unit of rotary jet. Finally, the field tests of engineering prototype were carried out in three wells to verify the stability and effectiveness of the prototype.

2 Mechanism of wellbore strengthening

The following assumptions are adopted: (a) the rock is homogeneous linear elastic porous medium; (b) the crack is a vertical micro crack and biplane symmetrical distribution; (c) considering the symmetrical distribution crack shape into a part of the flat ellipse, as shown in Fig. 2.

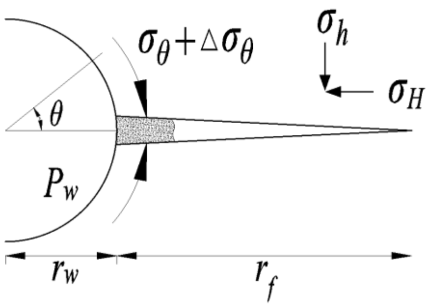

Fig. 2. Stress analysis of sketch of stress cage.

According to the continuum mechanics theory, the tangential stress unaffected by invading fluid or the presence of the fracture is given by the Kirsh equation (Lee et al., 2004):

$$\sigma_\theta = \sigma_h + \left[\frac{1}{2}(\sigma_H + \sigma_h) - P_w\right]\left(\frac{r_w}{r}\right)^2 - \frac{3}{2}(\sigma_H - \sigma_h)\left(\frac{r_w}{r}\right)^4 \tag{1}$$

$$\sigma_r = P_w \tag{2}$$

where σ_θ is the circumferential stress; σ_H and σ_h are the maximum and minimum horizontal principal stresses, respectively; σ_r is the radial stress; r_w is the radius of wellbore; r is the radial distance measured from the borehole centerline; P_w is the pressure in the borehole.

If the fracture is vertical and propagates perpendicular to the minimum horizontal stress, in the vicinity of a vertical borehole the net pressure may be written as:

$$\Delta p = p_{frac} - \sigma_\theta \tag{3}$$

where Δp is the net pressure; p_{frac} is the pressure inside the fracture.

The goal of wellbore strengthen is to reduce net pressure by increasing closure stress (hoop stress enhancement mechanism) or decreasing the averaged traction applied at the fracture surface after seal-off the crack (propagation resistance mechanism) (Zhao et al., 2017). After the effect of rotary jet, a filter cake with different shape, location and intensity will be formed inside the crack depending on the size and property of the lost circulation material (LCM). Compared with the initial state of fracture (no filter-cake plugging with clear fluid), the filter cake formed by the proposed tool will conduct both mechanisms to reduce net pressure to strengthen the wellbore. Considering the uncertainty and complexity of the shape, location and intensity of the filter cake, it is difficult to calculated the pressure in the crack. At the same time, it is thought the crack heals itself after sealing by the plugging agent, and the crack opens again if lost circulation occurs, without paying attention to the morphology and extension of the crack. Therefore, only the influence of circumferential stress increment $\Delta\sigma_\theta$ (i.e. closure stress increment) on the collapse, fracture burst pressures and the drilling mud-weight window is analyzed. This closure stress increment $\Delta\sigma_\theta$ increment is the result of filter cake and pressure distribution in the crack. Thus, Eq. (1) is converted to:

$$\sigma_\theta = (1 - 2\cos2\theta)\sigma_H + (1 + 2\cos2\theta)\sigma_h - P_w \tag{4}$$

The Mohre-Coulomb and the maximum tension stress criterions are adopted to judge the instability and fracture burst of the formation:

$$\tau_0 = \frac{\sigma_1}{2}\left(\sqrt{f^2+1} - f\right) - \frac{\sigma_3}{2}\left(\sqrt{f^2+1} + f\right) \tag{5}$$

$$\sigma_\theta = -\sigma_t \tag{6}$$

where τ_0 is the cohesion of rock; φ is the internal friction angle; σ_t is the tensile strength.

Contrast the equations of wellbore stress component (2) and (4) with the Mohre-Coulomb and maximum tension stress criterions, considering the influence of circumferential stress increment $\Delta\sigma_\theta$, the collapse and fracture burst pressures at different positions of borehole wall can be calculated by the following equations:

$$P_c = \frac{f_1[(1-2\cos 2\theta)\sigma_H + (1+2\cos 2\theta)\sigma_h + \Delta\sigma_\theta] - 2\tau_0}{f_1 + f_2} \tag{7}$$

$$P_f = [(1-2\cos 2\theta)\sigma_H + (1+2\cos 2\theta)\sigma_h + \Delta\sigma_\theta] + \sigma_t \tag{8}$$

where σ_t is the tensile strength of rock; P_c, P_f are the collapse and fracture burst pressures at different positions of borehole wall; $f_1 = \sqrt{f^2+1} - f$, $f_2 = \sqrt{f^2+1} + f$, $f = \tan\varphi$.

Fig. 3 shows the effect of circumferential stress increment $\Delta\sigma_\theta$ on the collapse and fracture burst pressures of the borehole Wall. The collapse and fracture burst pressure increase with increasing $\Delta\sigma_\theta$. The increase of fracture burst pressure is in favor of wellbore strengthening, while the increase of collapse pressure is bad for borehole wall stability. Fig. 4 shows the effect of $\Delta\sigma_\theta$ on drilling mud-weight window under different in-situ stress anisotropy. From Fig. 4, the mud-weight window increases with increasing $\Delta\sigma_\theta$ under different in-situ stress anisotropy. The mud-weight window increment (the difference between the MWW with and without $\Delta\sigma_\theta$) increases with increasing $\Delta\sigma_\theta$.

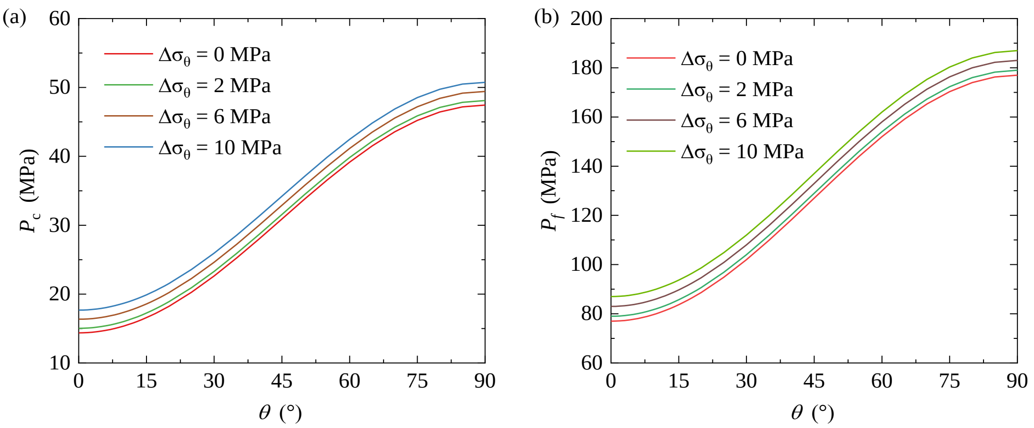

Fig. 3. Effect of $\Delta\sigma_\theta$ on collapse and fracture burst pressures. (a) Collapse pressure P_c; (b)

Fracture burst pressure P_f. ($\frac{\sigma_H}{\sigma_h}$ = 1.5, σ_h = 50 MPa, τ_0 = 6 MPa, φ = 0.76 rad, σ_t = 2 MPa).

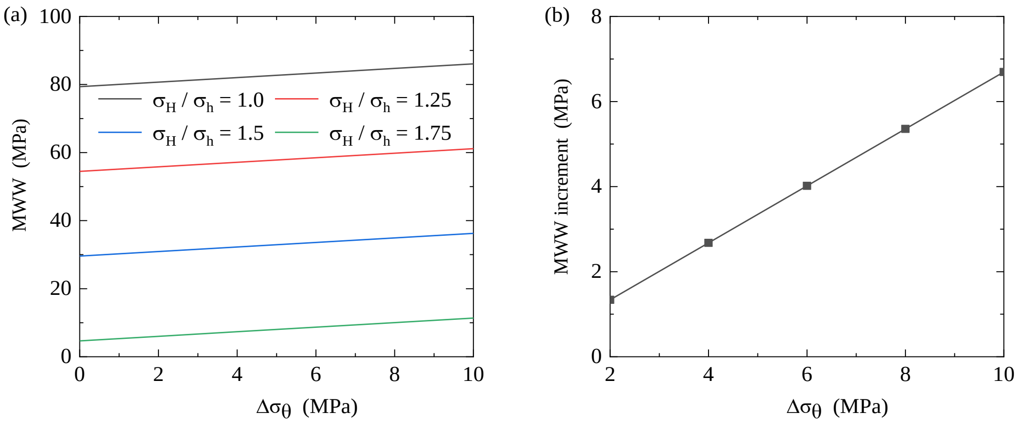

Fig. 4. Effect of $\Delta\sigma_\theta$ on drilling mud-weight window (MWW) under different in-situ stress anisotropy. (a) MWW; (b) MWW increment.

Based on the above analysis, the most important effect of rotary jet modulated by the proposed tool is to accelerate the formation of filter cake. The crack is sealed and widened by the filter cake, which makes it more difficult to re-open by increasing the closure stress (i.e. hoop stress enhancement mechanism). On the other hand, the pressure behind the filter cake in the crack gradually reduces from the borehole pressure to the pore pressure, which is equivalent to improve the usable borehole pressure (propagation resistance mechanism) (Zhao et al., 2017).

3 Rotary jet plugging tool

3.1 Structure design

The rotary jet plugging tool suitable for 8½″ borehole is designed in the High-pressure Water Jet Research Center of China University of Petroleum in China. The overall structure of the tool is shown in Fig. 5. The lower end of the tool with a 4½REG internal thread is designed to connected directly with the drill bit. The upper end of the tool with a 4½REG internal thread connects with drill-string. The outer and inner diameters of the tool are 160 mm and 75 mm, respectively. The outer diameter of the reinforce section ranges from 180 mm to 190 mm, and the side view of the reinforce section is a square with side length of 140 mm. The length of the tool ranges from 450 mm to 500 mm. The lateral rotary jet nozzles are the core elements of the tool. The fixed guide vanes in the nozzles are selected as the way to generate the rotary jet, that is, the flow direction of drilling fluid is changed by the guide vane, so that the pure axial flow becomes a rotary jet with three-dimensional velocity. The lateral nozzle diameter is constrained by the hydraulic energy of drill bit, here, the lateral displacement accounts for 15% of the total displacement of drilling pump, i.e. the diameter of nozzle of rotary jet tool equals one half the diameter of drill bit nozzle $d_r = 0.5d_b$. Other structural parameters: diameter of lateral liquid channel of rotary jet tool D = 24 mm; length of exit section, contraction section and blade are L_o = 5 mm, L_s = 10 mm and L = 16 mm; wheel hub diameter of blade d = 8 mm; guided angle of the blade β = 70° and the number of blades is three. The cone angle of the contraction section equals 80°.

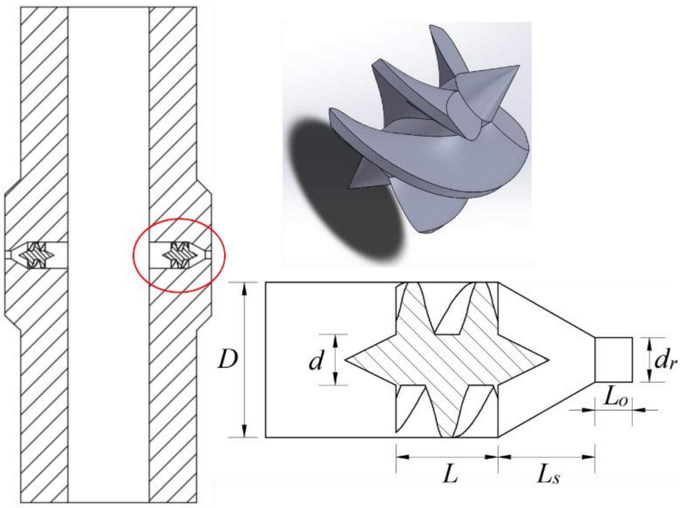

Fig. 5. Schematic diagram of the rotary jet tool and nozzle.

3.2 Optimization of structural parameters

3.2.1 Numerical model

The mixture multiphase flow model in Fluent software, which follow the Euler-Euler approach, were used to calculate the multiphase flow fields of the rotary jet with plugging particles. The relative velocity $\vec{v}_{qp}$ between dispersed phase and primary phase is given by

$$\vec{v}_{qp} = \tau_{qp}\vec{\alpha} \tag{9}$$

$$\vec{\alpha} = \vec{g} - \vec{v}_m \cdot \nabla \vec{v}_m - \frac{\partial \vec{v}_m}{\partial t} \tag{10}$$

$$\tau_{qp} = \frac{(\rho_m - \rho_p) d_p^2}{18 \mu_q f_d} \tag{11}$$

where $\vec{\alpha}$ is the acceleration of a dispersed bubble, m/s^2; τ_{qp} is the relaxation time of a dispersed bubble, s; f_d is the drag force, N.

Based on the continuity equation of the primary phase, the volume fraction equation of bubbles is given as

$$\frac{\partial}{\partial t}(\alpha_p \rho_p) + \nabla \cdot (\alpha_p \rho_p v_m) = -\nabla \cdot (\alpha_p \rho_p v_{dr,p}) \tag{12}$$

where α_p is the volume fraction of the bubble. The mean quality velocity $\vec{v}_m$ is defined as $\vec{v}_m = \frac{\sum_{k=1}^{n} \alpha_k \rho_k \vec{v}_k}{\rho_m}$, m/s. The drift velocity $\vec{v}_{dr,p}$ is given by $\vec{v}_{dr,p} = \vec{v}_p - \vec{v}_m$, m/s.

The $k - \varepsilon$ model is utilized to illustrate the turbulence and close the equations, which is appropriate for compressible fluid flow.

$$\begin{cases} \dfrac{\partial(\rho k)}{\partial t} + \dfrac{\partial}{\partial x_j}\left(\rho u_j \dfrac{\partial k}{\partial x_j} - (\mu + \mu_\tau)\dfrac{\partial k}{\partial x_j}\right) = \tau_{tij} S_{ij} - \rho\varepsilon + Q_k \\ \dfrac{\partial(\rho\varepsilon)}{\partial t} + \dfrac{\partial}{\partial x_j}\left(\rho u_j \varepsilon - \left(\mu + \dfrac{\mu_\tau}{1.3}\right)\dfrac{\partial \varepsilon}{\partial x_j}\right) = 1.45\dfrac{\varepsilon}{k}\tau_{tij} S_{ij} - 1.92 f_2 \rho \dfrac{\varepsilon^2}{k} + Q_\varepsilon \end{cases} \tag{13}$$

where $\tau_{tij} = 2\mu_\tau\left(S_{ij} - \frac{S_{nn}\delta_{ij}}{3}\right) - 2\rho k \delta_{ij}/3$ and the eddy viscosity $\mu_\tau = 0.09 f_u \rho k^2/\varepsilon$. The near wall attenuation functions are given as $f_u = e^{(-3.4/(1+0.02\mathrm{Re}_t)^2)}$ and $f_2 = 1 - 0.3e^{(-\mathrm{Re}_t^2)}$, where $\mathrm{Re}_t = \frac{\rho k^2}{\mu\varepsilon}$. The wall terms are given as $Q_k = 2\mu(\frac{\partial\sqrt{k}}{\partial y})^2$ and $Q_\varepsilon = 2\mu\frac{\mu_\tau}{\rho}(\frac{\partial^2 \mu_\varepsilon}{\partial y^2})^2$. S_{ij} stands for the mean-velocity strain-rate tensor, and δ_{ij} stands for the Kronecker delta (Stoesser and Nikora, 2008).

Simple arithmetic is adopted to solve the coupling of pressure and velocity. The inlet boundary is velocity inlet and the inlet velocity is 7 m/s (corresponding to displacement of 30 L/s). The volume fraction of particle phase of $CaCO_3$ is 5%. The outlet boundary is pressure outlet and the outlet pressure is 20 MPa. Considering the symmetry of the rotary jet plugging tool, take one half as computing area and use a polyhedron for mesh division and add a boundary layer. The total number of grids is 5870,275 (see Fig. 6).

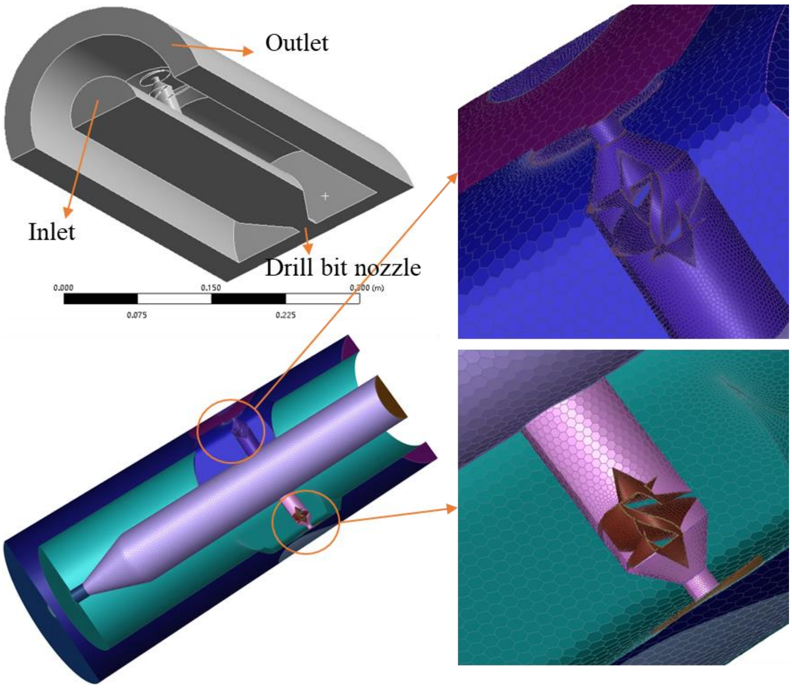

Fig. 6. Boundary conditions and meshing of one half the rotary jet tool.

3.2.2 Flow field characteristic

The effect action area and the additional impact pressure of the rotary jet were selected as the optimal indexes, and the dimensions of several important parameters (see Fig. 5, including: blade rotation angle γ, blade length L, contraction section length L_s, nozzle diameter d_r and lateral channel diameter D) of the rotary jet modulation tool were optimized by numerical simulation. The diameter of the lateral channel was fixed D = 24 mm and the remaining four parameters were analyzed through orthogonal test, as shown in Table 1. The pressure field contour of the lateral rotary jet impacting the borehole was shown in Fig. 7. It can be seen from Fig. 7, the additional impact pressure of rotary jet on borehole wall is less than 1.5 MPa. Considering that the safety window of drilling pressure is greater than 10MPa in most cases, we can conclude that the impact pressure of the rotary jet will not damage the borehole wall under simulating parameters. In addition, the action areas all exceed 250mm^2, which satisfy the requirement that the action radius exceeds 6mm. Except for the fourth and the eighth groups forming ring action regions, the results of other groups were all within a reasonable range. The reason for the ring action regions is that the curl of the rotary jet is relatively large, which can be improved by reducing the guide angle of blade β (by reducing the blade rotation angle γ or increasing the blade length L) or the cone angle of the contraction section (by increasing the length of the contraction section L_s).

Table 1 Orthogonal design table and simulation results.

No.	γ (°)	L (mm)	L_s (mm)	d_r (mm)	Action area (mm²)	Highest impact pressure (MPa)
1	150°	14	10	6	258.11	21.22
2	150°	16	12	7	318.88	21.12
3	150°	18	14	8	375.12	20.98
4	180°	14	12	8	451.15	20.31
5	180°	16	14	6	250.64	21.45
6	180°	18	10	7	341.46	20.82
7	210°	14	14	7	373.41	20.38
8	210°	16	10	8	443.27	20.31
9	210°	18	12	6	256.83	21.19

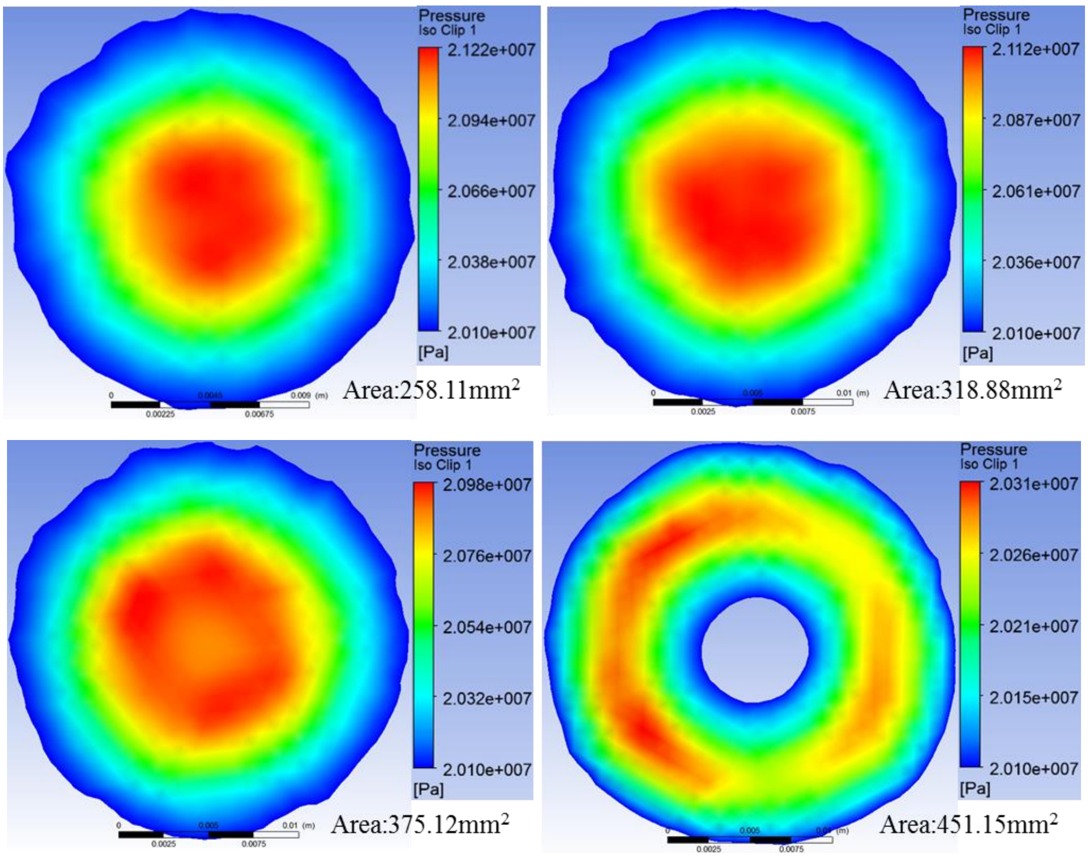

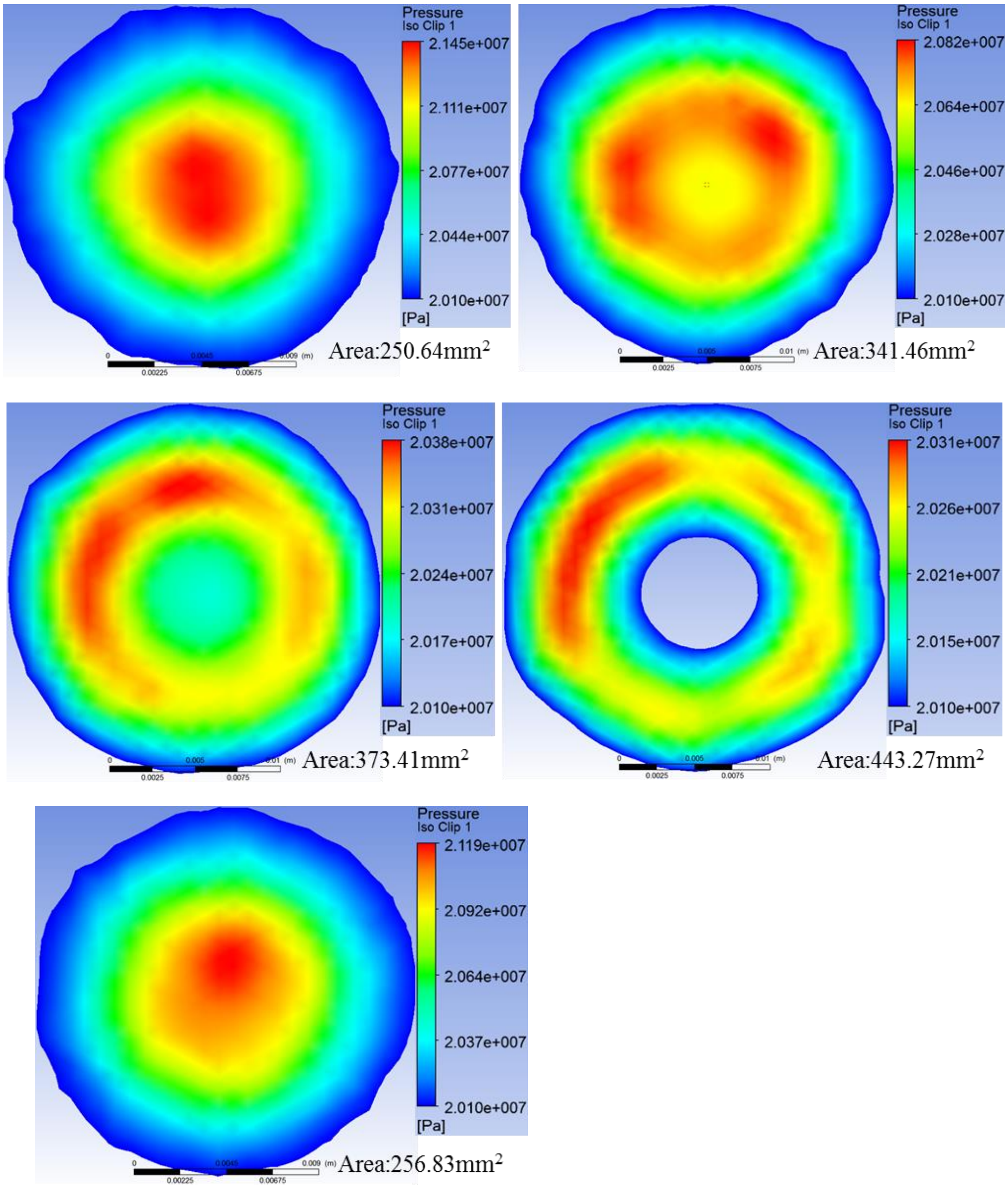

Fig. 7. Pressure contour of the lateral rotary jet impacting the borehole wall (> 20.1 MPa was chosen as the effective action area).

The range analysis was carried out with the action area and additional impact pressure as indicators respectively, and obtained the influence of factors increased in the order of contraction section length L_s, blade length L, blade rotation angle γ, and nozzle diameter d_r. The optimal assembly of structure parameters is d_r = 7 mm, φ = 150°, L = 14mm and L_s = 12mm. Next, the influence of lateral channel diameter on the action area and impact pressure was investigated by controlling variables. The experimental scheme and simulation results were shown in Table 2 and Fig. 8. It can be seen from the simulation results that the action area decreased and the additional impact pressure increased with increasing lateral channel diameter.

Table 2 Effect of rotary jet under different lateral channel diameter.

No.	D (mm)	Action area (mm^2)	Highest impact pressure (MPa)
1	24	334.26	20.77
2	26	318.83	21.07
3	28	314.23	21.36

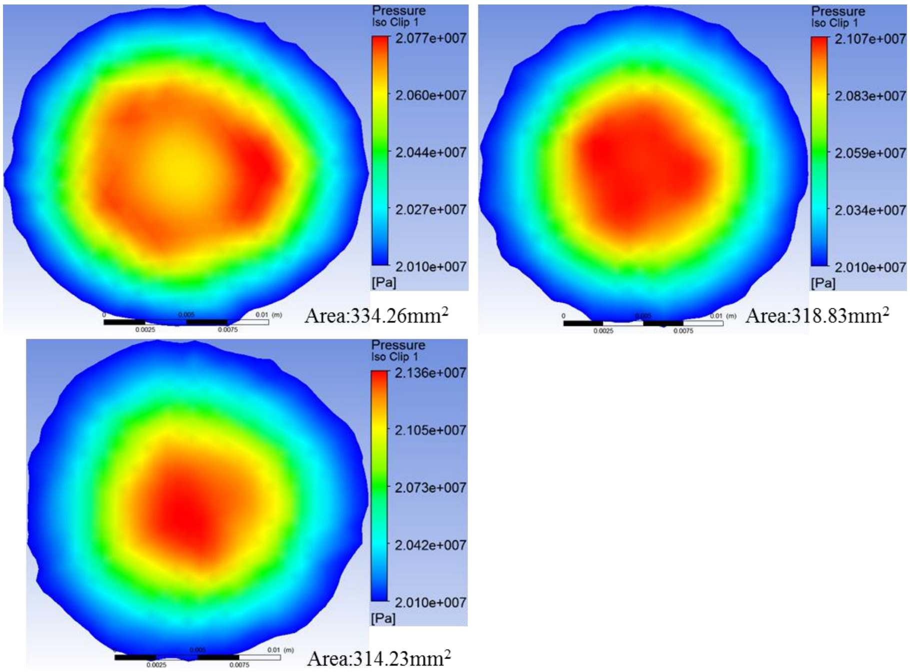

Fig. 8. Pressure contour of the lateral rotary jet impacting the borehole wall under different lateral liquid channel diameter (> 20.1 MPa was chosen as the effective action area).

The influence law of five main structural parameters on the action area and additional impact pressure of rotary jet is shown in Table 3. From the perspective of reducing the water power consumption of drill bit, the lateral channel diameter is better to take a smaller value. Meanwhile, we need larger lateral channel diameter to improve the additional impact force. The lateral channel diameter is set as D = 26 mm through comprehensive consideration. According to above structural parameters, an engineering prototype of rotary jet plugging toll is developed 35CrMo alloy steel, as is shown in Fig. 9.

Table 3 Influence of main structural parameters on the jet effect.

Factors		Action area	Additional impact pressure
Blade rotation angle γ	↑	↑	↓
Blade length L	↑	↓	↑
Contraction section length L_s	↑	↓	↑
Nozzle diameter d_r	↑	↑	↓
Lateral channel diameter D	↑	↓	↑

Fig. 9. Engineering prototype of rotary jet plugging tool.

4 Field tests

The field tests of engineering prototype were carried out in 8½″ interval of three wells: Dingbei 30, Fuping exploratory well 1 and LP14H of Shengli oilfield in Bohai Bay Basin of China. The stratum formation and drilling parameters of test wells are shown in Table 4. The bottom hole assemblies of well Dingbei 30 and Fuping 1 are the same: a PDC drill bit 215.9 mm in diameter + Rotary jet tool 178mm in diameter + a non-magnetic drill collar 177.8 mm in diameter + a helical centralizer 214 mm in diameter + seven drill collars 177.8 mm in diameter + thirty heavy weight drill pipe 127 mm in diameter + a lot of drill pipe 127 mm in diameter. The bottom hole assembly of well LP14H is: a PDC drill bit 215.9 mm in diameter + Rotary jet tool 178mm in diameter + a back-pressure valve + a non-magnetic drill collar 177.8 mm in diameter + a drill collar 177.8 mm in diameter + a helical centralizer 214 mm in diameter + eight drill collars 177.8 mm in diameter + seventeen heavy weight drill pipe 127 mm in diameter + a lot of drill pipe 127 mm in diameter. The components of drilling fluid for preventing lost circulation of the three wells are the same: 5% SDL (150 mesh) +5% SQD-98 (180 mesh) + 5% SQD-98 (120 mesh) + 5% walnut shell (10 mesh) + 3% walnut shell (5 mesh) + 2% asphalt + 5% QS-2 (400 mesh).

Table 4 Stratum information and drilling parameters of test wells.

Well name		Dingbei 30	Fuping 1	LP14H
Test interval (m)		3095~3546	2025~2374	2959~3213
Test stratum		Liujiagou, shiqianfeng and shihe blocks	Liujiagou block	Liujiagou and shiqianfegn blocks
Drilling parameter	WOB (KN)	120~140	80~120	60~120
	Displacement (L/s)	32	30~34	28~31
	Stand pipe pressure (MPa)	15	11	13
	Rotate speed (r/min)	60	80	50~70
Density of drilling fluid (g/cm^3)		1.23	1.25	1.26
Maximal temperature (°C)		90	63	75.2
Circulation time (h)		131.5	113	63.75
Drilling time (h)		113	89	52.84

The pressure-bearing capacity of test wellbores after using rotary jet plugging technology are shown in Fig. 10. In order to test the wellbore strengthening effect of rotary jet tool, a higher drilling fluid density was used in the three test wells. The density of drilling fluid of well Dingbei 30 in test interval was 1.23 g/cm^3 and no lost circulation happened. In contrast, the lost circulation happened when the drilling fluid density equaled 1.02g/cm^3 in the same stratum of offset well Dingbei 28, which was 3320 m from well Dingbei 30 as the crow flies. The density of drilling fluid of well Fuping 1 in test interval was 1.25 g/cm^3 and no lost circulation happened, in contrast, the lost circulation happened when the drilling fluid density equaled 1.02g/cm^3 in the same stratum of offset well Fugu 7, which was only 7 m from well Fuping 1 as the crow flies. And the density of drilling fluid of well LP14H in test interval was 1.26 g/cm^3 and no lost circulation happened, in contrast, the lost circulation happened when the drilling fluid density equaled 1.02 g/cm^3 in the same stratum of offset well LP1T, which was only 4510 m from well LP14H as the crow flies. The application results of the three wells indicated that the rotary jet plugging tool could be used over 130 hours without maintenance, which verified the reliability of the tool. On the other hand, no lost circulation happened after improving the density of drilling fluid to a relatively high level, which verified the wellbore strengthening was improved by usage of rotary jet tool. It's important to note that the improvement of drilling fluid density was limited to the 0.21 ~ 0.24 g/cm^3 range mainly due to the negative effect of high density on rate of penetration and the risk of well leak.

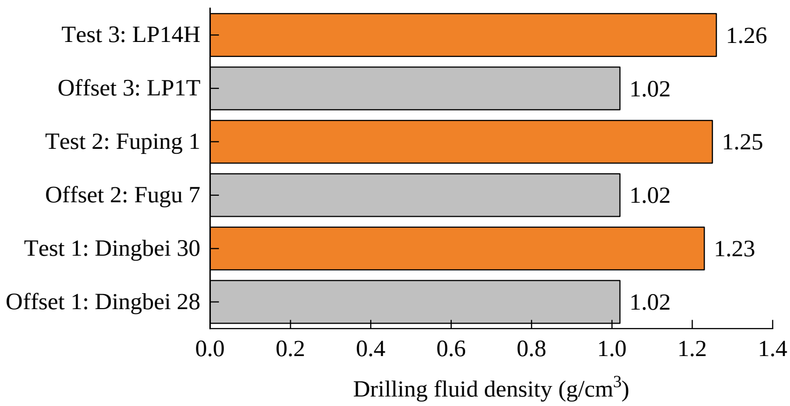

Fig. 10. Pressure-bearing capacity of test wellbore after using rotary jet plugging technology.

Conclusions

The mechanism and application of mitigating lost circulation and wellbore strengthening of rotary jet while drilling were studied in this paper, the following conclusions were obtained:

(1) A stress analysis model based on elastic-plastic mechanics was established to reveal the wellbore strengthening mechanism of rotary jet plugging technology while

drilling: the particle materials rapidly rush to the crack at different angles, enrich at the crack entrance and quickly form sealing under the action of rotating jet. The transmission of drilling fluid pressure to the crack tip is effectively isolated and the crack expanding is prevented. The existence of circumferential stress increment makes the stress of the crack surface increases and the borehole wall more stable due to 'stress cage effect'.

(2) One type structure of rotary jet tool was proposed and obtained the influence law of the rotary jet nozzle structure parameters on the wellbore strengthening effect. The optimization design method of the rotary jet plugging tool was established, which lay a foundation for the further optimization of rotary jet tools.

(3) An engineering prototype of rotary jet tool, suitable for 8½″ wellbore, were developed and tested in three wells in Bohai Bay Basin of China. Satisfactory wellbore strengthening results verify the stability of prototype and effectiveness of rotary jet plugging and wellbore strengthening technology.

Nomenclature

σ_H	Maximum horizontal principal stress
σ_h	Minimum horizontal principal stress
σ_r	Radial stress of wellbore
σ_t	Tensile Strength of rock
σ_θ, $\Delta\sigma_\theta$	Circumferential stress of wellbore wall and circumferential stress increment, respectively
Δp	Net pressure
p_{frac}	Pressure inside the fracture
P_w	Pressure in the borehole.
r	Radial distance measured from the borehole centerline
r_w	Radius of wellbore
r_f	Distance between the crack tip and center of wellbore
τ_0	Cohesion of rock

φ	Internal friction angle
d	Wheel hub diameter of blade
d_b	Equivalent diameter of nozzle of drill bit
d_r	Diameter of nozzle of rotary jet tool
D	Diameter of lateral liquid channel of rotary jet tool
L_o, L_s, L	Length of exit section, contraction section and blade, respectively
γ	Blade rotation angle
β	Guide angle of the blade
P_c, P_f	Collapse and fracture burst pressures at different positions of wellbore

Acknowledgments

The authors gratefully acknowledge the financial support of the National Natural Science Foundation of China (Grant No. 51704323), Qingdao headstream innovation and applied basic research project (Grant No. 19-6-2-22-cg), and the Fundamental Research Funds for the Central Universities (Grant No. 20CX02322A, 18CX02072A), in part by the Opening Fund of National Engineering Laboratory of Offshore Geophysical and Exploration Equipment. The authors express their appreciation for the comments of the anonymous reviewers and the editors.

References

Alberty, M.W. and McLean, M.R., 2001. Fracture Gradients in Depleted Reservoirs - Drilling Wells in Late Reservoir Life, SPE/IADC Drilling Conference. Society of Petroleum Engineers, Amsterdam, Netherlands, pp. 8.

Alberty, M.W. and McLean, M.R., 2004. A Physical Model for Stress Cages, SPE Annual Technical Conference and Exhibition. Society of Petroleum Engineers, Houston, Texas, pp. 8.

Carpenter, C., 2014. Liner-Drilling Technology Mitigates Lost Circulation Offshore Mexico. SPE-14262-PA, 66(06): 104-107.

Dupriest, F.E., 2005. Fracture Closure Stress (FCS) and Lost Returns Practices, SPE/IADC Drilling Conference. Society of Petroleum Engineers, Amsterdam, Netherlands, pp. 11.

Dupriest, F.E., Smith, M.V., Zeilinger, S.C. and Shoykhet, N., 2008. Method To Eliminate Lost Returns and Build Integrity Continuously With High-Filtration-Rate Fluid, IADC/SPE Drilling Conference. Society of Petroleum Engineers, Orlando, Florida, USA, pp. 10.

Feng, Y., Jones, J.F. and Gray, K.E., 2016. A Review on Fracture-Initiation and -Propagation Pressures for Lost Circulation and Wellbore Strengthening. SPE-145765-PA, 31(02): 134-144.

Feng, Y.C. and Gray, K.E., 2017. Review of fundamental studies on lost circulation and wellbore strengthening. J. Pet. Sci. Eng., 152: 511-522.

Fuh, G.-F., Beardmore, D.H. and Morita, N., 2007. Further Development, Field Testing, and Application of the Wellbore Strengthening Technique for Drilling Operations, SPE/IADC Drilling Conference. Society of Petroleum Engineers, Amsterdam, The Netherlands, pp. 12.

Fuh, G.-F., Morita, N., Boyd, P.A. and McGoffin, S.J., 1992. A New Approach to Preventing Lost Circulation While Drilling, SPE Annual Technical Conference and Exhibition. Society of Petroleum Engineers, Washington, D.C., pp. 14.

Green, A.E. and Sneddon, I.N., 1950. The distribution of stress in the neighbourhood of a flat elliptical crack in an elastic solid. Mathematical Proceedings of the Cambridge Philosophical Society, 46(1): 159-163.

Lee, D., Bratton, T. and Birchwood, R., 2004. Leak-Off Test Interpretation And Modeling With Application To Geomechanics, Gulf Rocks 2004, the 6th North America Rock Mechanics Symposium (NARMS). American Rock Mechanics Association, Houston, Texas, pp. 13.

Mehrabian, A., Jamison, D.E. and Teodorescu, S.G., 2015. Geomechanics of Lost-Circulation Events and Wellbore-Strengthening Operations. SPE-174088-PA, 20(06): 1305-1316.

Morita, N., Black, A.D. and Guh, G.F., 1990. Theory of Lost Circulation Pressure, SPE Annual Technical Conference and Exhibition. Society of Petroleum Engineers, New Orleans, Louisiana, pp. 16.

Morita, N. and Fuh, G.-F., 2012. Parametric Analysis of Wellbore-Strengthening Methods From Basic Rock Mechanics. SPE-145765-PA, 27(02): 315-327.

Morita, N., Whitfill, D.L. and Wahl, H.A., 1988. Stress-Intensity Factor and Fracture Cross-Sectional Shape Predictions From a Three-Dimensional Model for Hydraulically Induced Fractures. SPE-14262-PA, 40(10): 1329-1342.

Nair, R. and Abousleiman, Y., 2009. A Porothermoelastic Wellbore Model in Oil and Gas Saturated Naturally Fractured Porous Media, SPE Saudi Arabia Section Technical Symposium. Society of Petroleum Engineers, Al-Khobar, Saudi Arabia, pp. 29.

Onyia, E.C., 1994. Experimental Data Analysis of Lost-Circulation Problems During Drilling With Oil-Based Mud. SPE-145765-PA, 9(01): 25-31.

Palmer, I.D., 1993. Induced Stresses Due to Propped Hydraulic Fracture in Coalbed Methane Wells, Low Permeability Reservoirs Symposium. Society of Petroleum Engineers, Denver, Colorado, pp. 12.

Stoesser, T. and Nikora, V.I., 2008. Flow structure over square bars at intermediate submergence: Large Eddy Simulation study of bar spacing effect. Acta Geophysica, 56(3): 876-893.

Sweatman, R., Faul, R. and Ballew, C., 1999. New Solutions for Subsalt-Well Lost Circulation and Optimized Primary Cementing, SPE Annual Technical Conference and Exhibition. Society of Petroleum Engineers, Houston, Texas, pp. 11.

Sweatman, R., Wang, H. and Xenakis, H., 2004. Wellbore Stabilization Increases Fracture Gradients and Controls Losses/Flows During Drilling, Abu Dhabi International Conference and Exhibition. Society of Petroleum Engineers, Abu Dhabi, United Arab Emirates, pp. 15.

Sweatman, R.E., Kessler, C.W. and Hillier, J.M., 1997. New Solutions to Remedy Lost Circulation, Crossflows, and Underground Blowouts, SPE/IADC Drilling Conference. Society of Petroleum Engineers, Amsterdam, Netherlands, pp. 16.

van Oort, E., Friedheim, J.E., Pierce, T. and Lee, J., 2011. Avoiding Losses in Depleted and Weak Zones by Constantly Strengthening Wellbores. SPE-145765-PA, 26(04): 519-530.

Wang, H., Soliman, M.Y. and Towler, B.F., 2008. Investigation of Factors for Strengthening a Wellbore by Propping Fractures, IADC/SPE Drilling Conference. Society of Petroleum Engineers, Orlando, Florida, USA, pp. 15.

Wang, H., Soliman, M.Y., Towler, B.F. and Shan, Z., 2009. Strengthening a Wellbore With Multiple Fractures: Further Investigation of Factors For Strengthening a Wellbore, 43rd U.S. Rock Mechanics Symposium & 4th U.S. - Canada Rock Mechanics Symposium. American Rock Mechanics Association, Asheville, North Carolina, pp. 9.

Wang, H., Sweatman, R.E., Engelman, R.E., Deeg, W.F.J. and Whitfill, D.L., 2005. The Key to Successfully Applying Today's Lost Circulation Solutions, SPE Annual Technical Conference and Exhibition. Society of Petroleum Engineers, Dallas, Texas, pp. 15.

Wang, H., Towler, B.F. and Soliman, M.Y., 2007a. Fractured Wellbore Stress Analysis: Sealing Cracks to Strengthen a Wellbore, SPE/IADC Drilling Conference. Society of Petroleum Engineers, Amsterdam, The Netherlands, pp. 15.

Wang, H., Towler, B.F. and Soliman, M.Y., 2007b. Near Wellbore Stress Analysis and Wellbore Strengthening for Drilling Depleted Formations, Rocky Mountain Oil & Gas Technology Symposium. Society of Petroleum Engineers, Denver, Colorado, U.S.A., pp. 12.

Wang, Z., Yang, M.Z. and Chen, Y.H., 2019. Numerical modeling and analysis of induced thermal stress for a non-isothermal wellbore strengthening process. J. Pet. Sci. Eng., 175: 173-183.

Whitfill, D., 2008. Lost Circulation Material Selection, Particle Size Distribution and Fracture Modeling with Fracture Simulation Software, IADC/SPE Asia Pacific Drilling Technology Conference and Exhibition. Society of Petroleum Engineers, Jakarta, Indonesia, pp. 12.

Whitfill, D.L., 2005. Wellbore Pressure Containment. Society of Petroleum Engineers, pp. 40.

Whitfill, D.L. and Hemphill, T., 2003. All Lost-Circulation Materials and Systems Are Not Created Equal, SPE Annual Technical Conference and Exhibition. Society of Petroleum Engineers, Denver, Colorado, pp. 9.

Whitfill, D.L., Jamison, D.E., Wang, M. and Angove-Rogers, A., 2007. Preventing Lost Circulation Requires Planning Ahead, International Oil Conference and Exhibition in Mexico. Society of Petroleum Engineers, Veracruz, Mexico, pp. 4.

Whitfill, D.L., Jamison, D.E., Wang, M. and Thaemlitz, C., 2006. New Design Models and Materials Provide Engineered Solutions to Lost Circulation (Russian), SPE Russian Oil and Gas Technical Conference and Exhibition. Society of Petroleum Engineers, Moscow, Russia, pp. 14.

Zhao, P., Santana, C.L., Feng, Y. and Gray, K.E., 2017. Mitigating lost circulation: A numerical assessment of wellbore strengthening. Journal of Petroleum Science and Engineering, 157: 657-670.